# A Resource Allocation Mechanism for Cloud Radio Access Network Based on Cell Differentiation And Integration Concept

Zainab H. Fakhri*, M.Khan*, Firas Sabir, H.S. Al-Raweshidy, *Senior Member*, IEEE

**Abstract**—A Self-Organising Cloud Radio Access Network (C-RAN) is proposed, which dynamically adapt to varying capacity demands. The Base Band Units and Remote Radio Heads are scaled semi-statically based on the concept of cell differentiation and integration (CDI) while a dynamic load balancing is formulated as an integer-based optimisation problem with constraints. A Discrete Particle Swarm Optimisation (DPSO) is developed as an Evolutionary Algorithm to solve load balancing optimisation problem. The performance of DPSO is tested based on two problem scenarios and compared to an Exhaustive Search (ES) algorithm. The DPSO deliver optimum performance for small-scale networks and near optimum performance for large-scale networks. The DPSO has less complexity and is much faster than the ES algorithm. Computational results demonstrate significant throughput improvement in a CDI-enabled C-RAN compared to a fixed C-RAN, i.e., an average throughput increase of 45.53% and 42.102%, and a decrease of 23.149% and 20.903% in the average blocked users is experienced for Proportional Fair (PF) and Round Robin (RR) schedulers, respectively. A power model is proposed to estimate the overall power consumption of C-RAN. A decrease of $\approx 16\%$ is estimated in a CDI-enabled C-RAN when compared to a fixed C-RAN, both serving the same geographical area.

**Index Terms**—Base Band Unit (BBU), Cloud Radio Access Network (C-RAN), Particle Swarm Optimisation (PSO), Remote Radio Head (RRH), Self-Optimising Network (SON).

✦

## 1 INTRODUCTION

IN the past few years, the proliferation of personal hand-held mobile computing devices such as tablets and smartphones, along with the growing volume of data-demanding services and applications, has produced and a great need for wireless access and high-speed data transmission. Internet access anywhere and everywhere has triggered the formation of radio *hot-spot* networks. The major challenge in cellular networks is managing the available resources in a way to achieve 1) Optimum returns on investment, 2) User's service demands satisfaction, and 3) High levels of network QoS. Unaware of the cell load, a user equipment (UE) associates itself to the cell providing the strongest signal. The spatial distribution of users and their capacity demands vary with respect to time, causing unbalanced traffic loads and wasteful utilisation of network's resources. Therefore, it is important to self-optimise the network resources dynamically.

To overcome the aforementioned challenges, C-RAN [1]–[3] has been proposed as a novel architecture that can address some significant challenges the Mobile Network Operators (MNOs) are facing with today. C-RAN architecture is composed of three parts: 1) The Base Band Units (BBUs) collected into a virtualised BBU cloud/pool for centralised processing, 2)The Remotely distributed Remote Radio Heads (RRHs) in the radio access network, and 3) An optical transport network (OTN) that connects the BBUs to the RRH. C-RAN can achieve significant cost and energy savings by dynamically scaling the BBUs with respect to changing traffic conditions [4] and adjusting the logical BBU-RRH links using suitable resource allocations schemes.

C-RAN with Self-optimising ability can provide MNOs with a flexible network regarding network dimensioning, adaptation to non-uniform traffic, and efficient utilisation of network resources. However, before a full commercial C-RAN deployment, several challenges need to be addressed. Firstly, the front-haul technology used must support enough bandwidth for delivering delay sensitive signals. Secondly, the proper BBU-RRH assignment in C-RAN to not only support collaboration technology like Cooperative Multipoint Processing (CoMP) [5] but also enabling dynamic load balancing and power saving in the network.

The main motivation of this paper is to exploit the capacity routing ability of C-RAN by employing self-optimisation for efficient resource utilisation with high levels of QoS and a balanced network load. Inspired by the concept of cell splitting in biological sciences, a two-stage design is proposed for real-time BBU-RRH mapping and power saving in C-RAN. The main contributions of the proposed scheme is as follows:

1) The proposed mechanism monitors the load on each cell in a given geographical area and divides it into multiple small cells and vice versa if the load in a cell exceeds or falls a certain threshold.

2) The fitting number of BBUs required to serve all RRHs in the given geographical area is assigned based on the actual load on the network. A key challenge of initial BBU-RRH mapping before identifying an optimum BBU-RRH mapping is

also addressed.

3)    An Evolutionary Algorithm (EA) is proposed to find the optimum BBU-RRH configuration to balance the network load for enhanced QoS. Therefore, the resources can be utilised efficiently.

This paper is organised as follows: Section 2 presents a survey of related work. Section 3 presents the system model. Section 4 illustrates the formulation for dynamic BBU-RRH allocation problem; Section 5 presents the RRH clustering constraint; Section 6 presents the proposed C-RAN power model; Section 7 defines the CDI algorithm. Computational results are discussed in Section 8. Finally, the paper is concluded in Section 9.

## 2  RELATED WORK

Artificial Intelligence (AI) techniques facilitate a network to automatically re-configure system parameters for optimum network performance and adaptively learn necessary system parameters to perform upgrades and maintenance routines along with recovering from failures. Since AI, is the basis of self-organising and machine learning network technologies, it can lead to a significant paradigm shift by driving the ongoing efforts in next-generation wireless network (5G) standardisation [6].

Most recent studies on resource management in C-RAN mainly focus on schemes related to RRH-UE mapping and only limited work addresses the BBU-RRH configuration schemes. Some related works on the former schemes are briefly discussed in [7]–[9]. In [7], the authors propose a QoS-aware radio resource optimisation solution for maximising downlink system utility in C-RAN. User grouping, virtual base stations clustering, and beamforming for multiuser, multicell distributed MIMO networks were investigated. In line with this work, the authors of [8] propose an efficient resource allocation scheme in heterogeneous C-RAN. A weighted minimum mean square error (WMMSE) approach is used to solve network-wide beamforming vectors optimisation and identify proper RRH-UE clusters. Moreover, minimising the number of active BBUs is formulated as a bin packing problem for energy saving. The work of [9] expresses a mixed integer non-linear programming (MINLP) problem aiming joint RRH selection to minimise power consumption via beamforming, where the transport network power is determined by the set of active RRHs. Regarding the BBU pool in C-RAN, some studies are described in [10]–[13]. A joint-scheduling strategy for resource allocation in C-RAN is proposed in [14] where the time/frequency resources of multiple base stations are jointly optimised to schedule network users concurrently for network throughput improvement. However, the authors did not consider BBU-RRH mapping and focused mainly on joint scheduling in C-RAN .The authors of [10] initially investigated semi-static and adaptive BBU-RRH switching schemes for C-RAN. The authors of [11] then proposed a lightweight, scalable framework that utilises optimal transmission strategies via BBU-RRH reconfiguration to cater dynamic user traffic profiles. A dynamic BBU-RRH mapping scheme is introduced in [12] using a borrow-and-lend approach in C-RAN. Overloaded BBUs switch their supported RRHs to underutilised BBUs for a balanced network load and enhanced throughput. The authors of [13] propose a load balancing technique which considers load fairness as an optimisation problem. When the load fairness exceeds an alarming threshold, the given geographical area is divided into small compact zones based on an infinite optimisation formulation. The author's previous work address a blocking probability based load balancing problem in C-RAN via evolutionary algorithms [15]. However, power saving in C-RAN was not addressed.

Regarding other related work, there have been attempts to develop Network Function Virtualisation (NFV) and Software Defined Network (SDN) solutions for C-RAN [16]–[18]. Although SDN and NFV are not the primary focus of this paper, they are presented in this section for a complete introduction of C-RAN. Moreover, an in-depth review of the principles, technologies and applications of C-RAN describing innovative concepts regarding physical layer, resource allocation, and network challenges together with their potential solutions are highlighted in [1], [19]

To sum up, the existing resource allocation mechanisms does not take full advantage of the centralised BBU pool concept in C-RAN. This paper extends the scope of C-RAN by introducing the concept of Cell Differentiation and Integration (CDI) with dynamic BBU-RRH mapping for load balancing and efficient resource utilisation. The system model in this article allows combining self-optimising feature of SON and capacity routing ability of C-RAN for a more centrally managed network operations.

## 3  SYSTEM MODEL

### 3.1  Proposed C-RAN Architecture

A self-optimised C-RAN architecture is presented in Fig. 1. The BBUs are decoupled from the RRH and migrated to a centralised BBU-pool, whereas the RRHs are left on the cell sites. A SON controller is introduced inside the BBU cloud which monitors the BBU-pool resource utilisation as well as controlling the switch. Since an optical switch can only support one-to-one switching, soft switching (one-to-one and one-to-many) is enabled indirectly by using optical splitters and multiplexers [11]. The SON controller dynamically assigns BBU pool resources to the independent RRHs based on traffic demands. However, each BBU allocates its radio resources (PRBs) only to the RRHs assigned to it at a particular time.

At extremely low traffic load conditions, only a high power macro-BS serves the given geographical area. As the traffic load increases and the macro cell reaches its load limit, the geographic area is differentiated into **C** equally sized small cells serving the same coverage area. Each **C** cell can further differentiate into **c** more small cells by activating the CDI supporting RRHs deployed to accommodate capacity demands. The actual number of RRHs are determined by the coverage area, users density, and other environment-related factors. However, both **C** and **c** are considered to be seven as a reasonable example.

Furthermore, the CDI concept is realised by considering three tiers of RRHs deployment as shown in Fig. 2, i.e., tier-3 RRH deployment imitates a high-power base station serving a Macro cell as in traditional cellular systems.
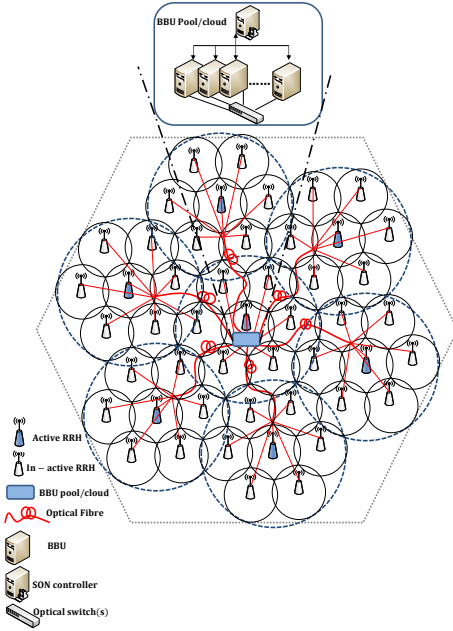
Fig. 1. Structure of a Cloud Radio Access Network represented as SON



Fig. 2. Cell differentiation and integration with multiple tiers of RRH deployment.

Tier-2 and tier-1 represents a structure with universal frequency reuse, where each cell is surrounded by a continuous tier of $6 + E$ and $6 \times [1 + j] + E$ cells, respectively. Where $E$ represents the number of other external macro cells and $j$ accounts for the level of differentiation. A set $\mathbf{S}_i = \{\text{RRH}_{i1}, \text{RRH}_{i2}, ..., \text{RRH}_{ic}\}$ is maintained for each cell $C_i$ in tier-2 RRH deployment, which contains a group of RRHs responsible for differentiating cell $C_i$ into $c$ small cells provided that the sum of transmit powers of all RRHs covers $C_i$ coverage area. The central RRH of each cell $C_i$ is represented as $\text{RRH}_{i1}$. Where $i$ represents the cell number in tier-2 RRH structure. The SON server is responsible for cell differentiation and integration with proper BBU-RRH configurations, whereas the optical switch is in charge of realising the settings via server commands. Note that, with small cell deployment in C-RAN, a high inter-cell interference is inevitable. Therefore, a clustering based interference mitigation technique is adopted to avoid network performance degradation. RRHs served by the same BBU are grouped together based on a proximity property [15].

### 3.2   Channel model

In this paper, Guaranteed Bit Rate (GBR) users with QoS requirements are considered. The frequency reuse factor is 1, and the time-frequency resources are equal for all BBUs. The basic unit of time-frequency resources that can be allocated to users per time slot (0.5 ms) of an LTE subframe is known as the Physical Resource Block (PRB). Each PRB consists of 12 consecutive sub-carriers with a sub-carrier spacing of 15 kHz, corresponding to 0.5 milli-seconds in time domain and 180 kHz in frequency domain. Let $\mathbf{M}$ and $\mathbf{N}$ represent the number of active BBUs and RRHs in the network, respectively, such that $\text{K}_{in}$ represents the total number of users in cell $i$ served by RRH $n$. Each user reports Channel Quality Information (CQI) to its serving BBU every two subframes (i.e., 2 milli-seconds) for proper PRB assignment.
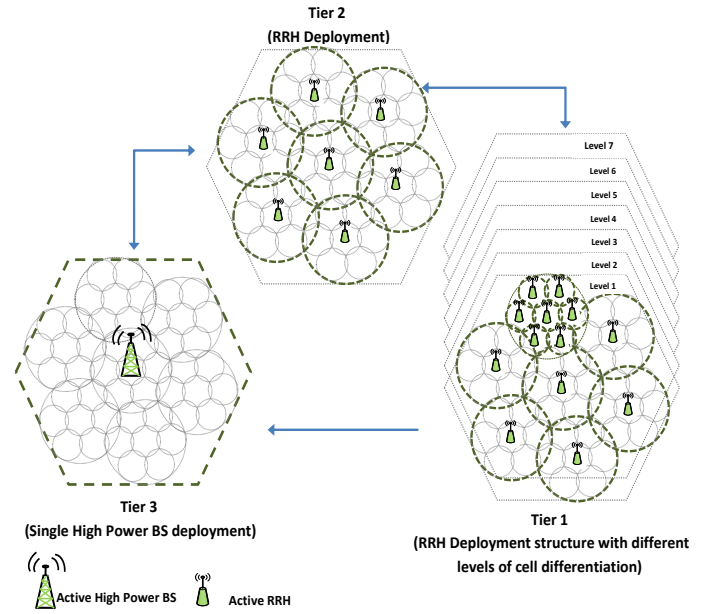
The channel model considered in this paper is a composite fading channel which involves path-loss and both small and large scale fading, given as:

$$\text{H}_{k_{in}} = \text{h}^*_{k_{in}} l_{k_{in}} \left[ \text{AD}_{k_{in}}^{-\delta} \right] \tag{1}$$

where $\text{h}^*_{k_{in}}$ and $l_{k_{in}}$ represent the small and large scale fading channel between the RRH $n$ and user $k$ in cell $i$, respectively. The small scale fading is assumed to be a Rayleigh random variables with a distribution envelop of zero-mean and unity-variance Gaussian process. $\text{AD}_{k_{in}}^{-\delta}$ reflects the path-loss between RRH $n$ and user $k$ in cell $i$, where A is a constant which depends on the carrier frequency $f_c$ and $\text{D}_{k_{in}}$ is the distance between user $k$ and RRH $n$ in cell $i$ and a path-loss exponent of $\delta$. In this paper, a path-loss of $(\text{A}, \delta) = (1.35 \times 10^7, 3)$ is considered [20] . The large scale fading is assumed to be lognormal random variable with a standard deviation of 10dB and is typically modelled with a probability density function of [21]:

$$\rho(l) = \frac{\zeta}{\sqrt{2\pi}\sigma_l l} \exp\left[ -\frac{\left(10\log_{10} l - \mu_l\right)^2}{2\sigma_l^2} \right] \tag{2}$$

where $\zeta = 10/\ln 10$, and $\mu_l$ and $\sigma_l$ are the mean and the standard deviation of $l$, both expressed in decibels.

The instantaneous Signal-to-Interference-and-Noise-Ratio $\gamma$ based on CQI received from user $k$ in cell $i$ served by RRH $n$ at time-slot $t$ is expressed as

$$\gamma_{k_{in}}(t) = \frac{\text{H}_{k_{in}}(t)\text{P}_{in}(t)}{\text{N}_0 + \sum_{j \in C} \sum_{a \in c, a \neq n} \text{H}_{k_{ja}}(t)\text{P}_{ja}(t)} \tag{3}$$

where $\text{P}_{in}(t)$ and $\text{H}_{k_{in}}(t)$ are the transmit power and channel gain between the serving RRH $n$ of user $k$ at time-slot $t$ in cell $i$ . $\text{N}_0$ is the power of Additive White Gaussian Noise per PRB and $\sum_{j \in C} \sum_{a \in c, a \neq n} \text{H}_{k_{ja}}(t)\text{P}_{ja}(t)$ represents the

inter-cell interference power received from all other active RRHs $a$ at time-slot $t$ in cells $j$ except the serving RRH $n$ of user $k$ in cell $i$.

Assuming the best modulation coding scheme, the highest data rate achieved by user $k$ served by $\text{RRH}_n$ in cell $i$ for a given SINR at time-slot $t$ can be expressed by Shannon formula:

$$\vartheta_{k_{in}}(t) = \log_2(1 + a\gamma_{k_{in}}(t)) \tag{4}$$

where $a$ is the constant bit error rate (BER) defined as $a = -1.5/ln(5 \times 10^{-6})$ [22]. The total PRB required by the user can be now be determined by the achievable throughput of the user $k$ at a given SINR, the demanded data rate $\phi_k$ of user $k$, and the bandwidth $\text{P}_{\text{BW}}$ of a single PRB (i.e., 180 KHz) from the following:

$$\text{N}_{\text{RB}}^k(t) = \left\lceil \frac{\phi_k(t)}{\text{p}_{\text{BW}}.\vartheta_{k_{in}}(t)} \right\rceil \tag{5}$$

where $\text{p}_{\text{BW}}$ represents the bandwidth of a PRB and the notion $\lceil . \rceil$ is the ceil function.

## 4 DYNAMIC BBU-RRH CONFIGURATION AND FORMULATION

For a Self-optimising C-RAN architecture shown in Fig. 1, it is essential to balance the network load amongst the active BBUs by proper BBU-RRH configuration. After each CDI cycle, the network may reconfigure itself by scaling the BBUs and RRHs with respect to traffic load. However, during the process, the BBU-RRH mapping might not satisfy the QoS requirement. Therefore, If the BBU-RRH configuration at time $t$ is known then it is necessary to adjust the BBU-RRH configuration at time $t + 1$ to adaptively balance the variance in traffic demands. Note that, the time between $t$ and $t + 1$ is longer than that of a subframe (i.e., one millisecond) and is called the load balancing cycle. A user location indicator vector $\mathbf{u} = \{u_1, u_2, ..., u_K\}$ is defined which shows users association with RRHs such that $u_k = \{r_{in}|r_{in} \in \mathbb{Z}^+ : i, n = 1, 2, 3, ...C\}$, where $u_k = r_{in}$ if user $k$ is associated with $\text{RRH}_n$ of cell $C_i$. To indicate RRHs association with BBUs, a vector $\mathbf{r} = \{r_{11}, r_{12}, ..., r_{in}\}$ is defined, where $r_{in} \in \{1, 2, ..., M\}$ and $r_{in} = m$ indicates $\text{RRH}_n$ of cell $C_i$ is being served by $\text{BBU}_m$. Whereas, $r_{in} = 0$ indicates that $\text{RRH}_n$ of cell $C_i$ is not active. If the user location indicator vector $\mathbf{u}$ is given, then the problem is to identify the new RRH allocation vector $\mathbf{r}$.

### 4.1 Number of BBUs required in the network

The required number of BBUs to serve the offered traffic load at a particular time $t$ can be calculated using actual load $\eta(t)$ on the network. Let $\eta_m(t)$ be the load on $\text{BBU}_m$ at time period $t$, which is represented as

$$\eta_m(t) = \frac{\sum_{k=1}^{K} \text{I}_{m,k}(t)\text{N}_{\text{RB}}^k(t)}{\text{P}_{\text{RB}}} \tag{6}$$

Where $\text{I}_{m,k}$ is a binary indicator such that $\text{I}_{m,k} = 1$ if user $k$ is served by $\text{BBU}_m$. However, an important constraint $\sum_{m=1}^{M} \text{I}_{m,k} = 1, \forall k$ defines that each user k is served by only one BBU at time period $t$. Note that, all BBUs are

assigned the same number of PRBs ($\text{P}_{\text{RB}}$). Another important constraint is that $\sum_{k=1}^{K} \text{I}_{m,k}(t)\text{N}_{\text{RB}}^k(t) \leq \text{P}_{\text{RB}}, \forall m$, which states that the number of PRBs assigned to users served by the same BBU should not exceed the BBU PRB limitation. The total load on the network at time $t$ is represented as the aggregated load on each active BBU at time $t$, which is given by

$$\eta(t) = \sum_{m=1}^{M} \eta_m(t) \tag{7}$$

Now the number of required BBUs (M) in the network at a particular time $t$ can be given as:

$$\text{No. of BBUs= M} = \begin{cases} \lceil \eta(t) \rceil & if \ \eta(t) < \text{M}_{\text{total}} \\ |\text{M}_{\text{total}}| & if \ \eta(t) \geq \text{M}_{\text{total}} \end{cases} \tag{8}$$

where $\text{M}_{\text{total}}$ is the total number of BBUs available in the BBU pool and the notation $\lceil . \rceil$ is the ceil function. Moreover, the load contributed by an active $\text{RRH}_n$ of cell $i$ in the network is given by

$$\eta_{\text{RRH}_{in}}(t) = \sum_{k=1}^{K} \text{I}_{k,in}(t)\text{N}_{\text{RB}}^k(t) \tag{9}$$

Network performance determined by Key Performance Indicators (KPIs). Based on these KPIs, the SON server identifies optimum BBU-RRH conguration by utilising the existing number of active BBUs and RRHs, to achieve a highly stable network with highest achievable QoS with respect to load demand. Following are the important KPIs considered for BBU-RRH mapping problem;

### 4.2 Key Performance Indicator for Load Fairness Index

In this paper, a Jains fairness index $\psi$ is monitored, which determines the level of load balancing in the network at a particular time $t$ and is defined as:

$$\psi(t) = \frac{\left(\sum_{m=1}^{M} \eta_m(t)\right)^2}{\text{M}\left(\sum_{m=1}^{M} \eta_m^2(t)\right)} \tag{10}$$

where M is the number of active BBUs. The range of $\psi$ is in the interval $[\frac{1}{M}, 1]$, with a higher value representing a highly balanced load distribution amongst all active BBUs. Therefore, maximising $\psi$ is one of the objectives to achieve a highly balanced load in the C-RAN.

### 4.3 Key Performance Indicator for Average Network Load

Minimising the average network load can avoid handovers of users with poor channel conditions in the system. A user(s) associated to an RRHs may have imperfect channel conditions with more PRBs requirement to meet desired data rate. Failure to meet the user's PRB demand, the BBU has to perform a handover operation. Therefore, to avoid unnecessary handovers, minimising the average network load is considered as a second objective and is given as

$$\eta_{ave}(t) = \frac{\sum_{m=1}^{M} \eta_m(t)}{\text{M}} \tag{11}$$

where $\eta_m(t)$ is the load on a $\text{BBU}_m$ defined in (6) and M is number of active BBUs calculated from (8).

## 4.4 Key Performance Indicator for Handovers

Network transition to a new BBU-RRH configuration may require significant forced handovers. An increased number of forced handovers in the system is undesirable and leads to performance degradation. Allocating an RRH to a new BBUs at a particular time results in forced handovers of all users associated with the RRH. Since inter-BBU handovers not only involves BBUs but a signalling overhead between the Serving Gateway (S-GW) and Mobility Management Entity (MME). Therefore, it is desirable to achieve a new optimum BBU-RRH configuration with a minimum required handovers. A handover index $h(t)$ is monitored as a third objective for load balancing problem and is given as:

$$h(t) = \frac{1}{2}\left(\frac{\sum_{m=1}^{M}\sum_{k=1}^{K}|I_{m,k}(t) - I_{m,k}^{\circ}(t)|}{K}\right) \quad (12)$$

where $I_{m,k}^{\circ}(t)$ is a binary variable that indicates a user's association to BBU in previous BBU-RRH configuration i.e., $I_{m,k}^{\circ}(t)=1$, if user $k$ is served by $\text{BBU}_m$ in previous BBU-RRH configuration.

## 5 RRH CLUSTERING

Proper BBU-RRH allocation can provide enhanced flexibility in C-RAN network management. However, an important limitation to consider is the reliable operation of C-RAN regarding BBU-RRH mapping for high system performances. Neighbouring RRHs must be assigned to the same BBU [12] to support advance LTE-A features like Coordinated MultiPoint transmission (CoMP) and to avoid unnecessary handovers among network cells. RRHs clustering is an approach to support CoMP for interference mitigation in LTE-A and C-RAN [23]. Therefore, this paper considers that the RRHs served by the same BBU forms a compact cluster. This compactness and consistently connected RRHs in a cluster, not only minimises frequent handovers among cells but also reduces the inter-cell interference among them. This is because compact an RRH group shares fewer common boundaries with other RRH groups. Therefore, the RRHs proximity is defined by introducing a binary variable $A_{ij}$, where $A_{ij}= 1$, if $\text{RRH}_i$ and $\text{RRH}_j$ are adjacent else $A_{ij}= 0$. If a cluster has multiple RRHs, then the RRHs in that cluster must be adjacent and connected. To formulate the connectedness of a cluster and proximity of the RRHs, let S1 be any proper subset of the set of RRHs served by $\text{BBU}_m$ ($Z_m$), such that $S1 \subset Z_m$, $S1 \neq \emptyset$, and $S1 \neq Z_m$. Let S2 be another subset of $Z_m$ such that, $S2 = Z_m - S1$, i.e., S2 is the complementary set of S1. To confirm that the RRHs in $Z_m$ are connected, the following property must be satisfied.

$$\sum_{i \in S1}\sum_{j \in S2} A_{ij} \geq 1 \quad (13)$$

For proper BBU-RRH configuration, a QoS function is needed which is the weighted combination of KPIs defined in (10), (11), and (12). The multiple objectives are combined into a single QoS objective function. This paper represents QoS as the following maximisation problem with constraints:

$$\text{Max}\quad \text{QoS}(t) = \alpha\psi(t) - \beta\eta_{ave}(t) - (1 - \alpha - \beta)h(t)$$

$$s.t.\quad C_1 : \sum_{i \in S1}\sum_{j \in S2} A_{ij} \geq 1, \forall S1,S2 \in Z_m, \forall m \in \{1, 2, ...M\}$$

$$C_2 : \sum_{k=1}^{K} I_{m,k}(t)N_{RB}^{k} \leq P_{RB}, \forall m \in \{1, 2, ...M\}$$

$$C_3 : \sum_{m=1}^{M} I_{m,k}(t) = 1, \forall k \in \{1, 2, ..., K\}$$

$$(14)$$

Both $\alpha$ and $\beta$ are control parameters of the QoS function. The main objective is to maximise the QoS function.

## 6 POWER MODEL FOR C-RAN

This section explains the necessary aspects needed to assess the power consumption of C-RAN. However, a more detailed description of the components involved in a C-RAN power model is given in [24]. The three most important parts considered for the power model are described as follows.

### 6.1 BBU Power estimation model

The BBU performs a different set of functions ($I_{BB}$) which includes scheduling of PRBs, Forward error correction, FFT and OFDM specific processing, filtering, modulation/demodulation, and transport link related functions, etc. These features can be measured in Giga Operations per Second (GOPS) and then translated into power figures. About 40 GOPS per Watt is estimated as the power cost of a large BBU [25]. The power model for the BBU can be given as:

$$P_{BBU} = \sum_{i \in I_{BB}} P_{i,BBU}^{ref} A^{x_i^A} W^{x_i^w} \quad (15)$$

where $P_{i,BBU}^{ref}$ in Watts represents the power consumption of BBU with respect to BBU functions. A is the number of antenna chains/RF transceivers with $x_i^A$ scaling exponent. W is the bandwidth share used in transmission with a scaling exponent $x_i^w$. In [26], the authors model BBU operations with exact scaling components and reference values to calculate BBU power consumption, shown in Table.1

### 6.2 RRH power estimation model

An RRH consist antenna chains/ RF transceivers, each with its own power amplifier (PA). The PA is main element of consideration as it consumes most of the power within an RRH. The power consumption of a PA is affected by its power efficiency ($\eta_{PA}$). The power consumed by the PA can be given as $P_{PA} = \frac{P_{TX}}{\eta_{PA}(\sigma_{feed})}$, where $P_{TX}$ is the output power of the PA, which depends on the bandwidth share ($\chi$), i.e., the actual number of physical resource blocks ($N_{RB}$) used for transmission and the output power of the antenna $P_{out}$ ($P_{TX} = P_{out}\chi$). $\sigma_{feed}$ represents the feeder loss. Moreover, the RF transceiver units of an RRH are responsible for functions like signal modulation/demodulation, voltage controlled oscillation and mixing, AC-DC and DC-AC conversions,

TABLE 1
BBU operations and their scaling values with transmit antennas and bandwidth

| Processing type, $i$ | GOPS | $P_{i,\text{BBU}}^{\text{ref}}$ [W] | $x_i^A$ | $x_i^w$ |
|---|---|---|---|---|
| Time Domain Processing | 360 | 9.0 | 1 | 0 |
| Frequency Domain Processing | 60 | 1.5 | 2 | 1 |
| Forward Error Correction | 60 | 1.5 | 1 | 0 |
| Central Processing Unit | 400 | 10.0 | 1 | 0 |
| Common Public Radio Interface | 300 | 7.5 | 1 | 0 |
| Leakage | 118 | 3.0 | 1 | 0 |



Fig. 3. Structure of a Cloud Radio Access Network represented as SON

and low noise, gain amplification. The power consumed by an RRH can be modelled as:

$$P_{\text{RRH}} = \sum_{a=1}^{A}(P_{\text{PA}} + P_{\text{RF}}) \tag{16}$$

where $a \in \{1, ..., A\}$ denotes the number of antenna/RF chains.

### 6.3 Optical transceiver power estimation model

In C-RAN architecture, the *front-haul* connectivity with high bandwidth, low cost, and low latency requirements for transport networks is challenging. Several factors influence the operation of optical transceivers such as the technology used, the operating conditions, and the output power required, which in turn affect the power consumption. From a power consumption perspective, the optical transceivers can be divided into two modules. The optical transmitter module, in which the OFDM electrical signals are modulated over optical carriers using an external or direct modulated lasers. And a receiver module which detects the optical OFDM signals either by direct detection or coherent detection. The power consumption of the optical transceiver as described in [27] can be given as:

$$P_{\text{TRANS}} = (P_{\text{laser}} + P_{\text{driver}} + P_{\text{I/O}})_{\text{TX}} + (P_{\text{PD}} + P_{\text{amp}} + P_{\text{I/O}})_{\text{RX}} \tag{17}$$

where $P_{\text{laser}}, P_{\text{driver}}, P_{\text{I/O}}, P_{\text{PD}},$ and $P_{\text{amp}}$ are the powers consumed by direct-modulated laser, electronics driving the laser, the electrical input/output interface, photodetector, and the trans-impedance and limiting amplifiers. This paper consider a point-to-point (PtP) transceivers rather than point-to-multipoint, because the PtP link loss is driven by distance and used operating wavelength only, i.e., the link loss of PtP is as low as 6dB with a 20 km network reach [28].

The total power consumption of a C-RAN ($P_{\text{C-RAN}}$) can be estimated by summing the power consumed by three main parts of the network along with power consumed by other components $P_{\text{OTHER}}$ such as power conversions(AC-DC, DC-DC) and cooling, i.e.,

$$P_{\text{C-RAN}} = \sum(P_{\text{BBU}} + P_{\text{TRANS}_B}) + \sum(P_{\text{RRH}} + P_{\text{TRANS}_R}) + P_{\text{OTHER}} \tag{18}$$

Where $P_{\text{TRANS}_B}$ and $P_{\text{TRANS}_R}$ indicates the power consumption of PtP transceivers located at each BBU and RRH, respectively. According to [29], base stations with a total power consumption $\leq 500$ Watts do not require a cooling system. This can be applied to RRH in C-RAN if its components (i.e., PA, RF, and optical transceiver) require an overall
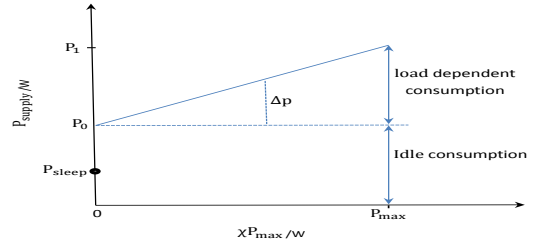
power less than 500 Watts. In this paper, the cooling power for RRH is ignored considering supply power as the only overhead.

From [24], the supply power required for a base station can be estimated as an affine function of transmitting power. The power consumption can be expressed by a load-dependant part that linearly increases with a power gradient (slope) $\Delta p$ and a static load independent part $P_{\text{static}}$ as shown in Fig. 3. Moreover, the supply power reaches a maximum $P_1$ when the transmitting power reaches the maximum limit $P_{\text{max}}$. A base station may enter an idle mode (sleep mode), with minimum power consumption ($P_{\text{sleep}}$) when it is not transmitting. The total supply power for a base station can be formulated as:

$$P_{\text{supply}}(\chi) = \begin{cases} P_1 + \Delta p \, P_{\text{max}}(\chi - 1) & \text{if } 0 < \chi \leq 1 \\ P_{\text{sleep}} & \text{if } \chi = 0 \end{cases} \tag{19}$$

where $P_1 = P_{\text{static}} + \Delta p \, P_{\text{max}}$. $\chi$ is a scaling parameter which indicates the bandwidth share, i.e., $\chi = 1$ indicates that the system is transmitting with full power and bandwidth whereas $\chi = 0$ represents an idle system. The basic power model presented in (19) is parameterised to understand the contribution of different parameters. Parameters which are assumed to be constant or having negligible effects are also highlighted. The following approximations are made:

• Both the BBU and Radio Frequency (RF) power consumption, linearly scales with the number of Antennas (A) and bandwidth (W), i.e., $P_{\text{BBU}} = A(\frac{W}{BW_{\text{TOTAL}}})P_{\text{BBU}}^{\text{pm}}$ and $P_{\text{RF}} = A(\frac{W}{BW_{\text{TOTAL}}})P_{\text{RF}}^{\text{pm}}$. Where $P_{\text{BBU}}^{\text{pm}}$ and $P_{\text{RF}}^{\text{pm}}$ are parameterised power consumption of BBU and RF, respectively.

• Each antenna unit of an RRH has a power amplifier (PA). The power consumed by a PA depends on the maximum power transmission per antenna unit ($\frac{P_{\text{max}}}{A}$) and its efficiency ($\eta_{\text{PA}}$). Losses between the antenna and PA are known as feeder losses ($\sigma_{\text{feed}}$) which may be ignored since PAs are placed close to the antennas [30].

• The loss factors of DC-DC, AC-DC conversions, main supply units (MS), and cooling power consumption for the BBU pool are approximated by $\sigma_{\text{DC,POOL}}, \sigma_{\text{MS,POOL}},$ and $\sigma_{\text{COOL,POOL}}$. Whereas for the RRHs, the loss factors are approximated by $\sigma_{\text{DC,RRH}}$ and $\sigma_{\text{MS,RRH}}$. Moreover, the optical fibre losses between BBUs and RRHs are approximated by a loss factor $\sigma_{\text{optical}}$.

• Power consumption of the optical transceivers linearly scales with the number of BBUs and RRHs.

If the power consumed by a single BBU serving a single RRH is:

$$P_1 = P_{BBU} + P_{RRH} \qquad (20)$$

$$P_1 = \frac{A(\frac{W}{BW_{TOTAL}})P_{BBU}^{pm} + P_{TRANS_B}}{(1 - \sigma_{DC,POOL})(1 - \sigma_{MS,POOL})(1 - \sigma_{COOL,POOL})}$$
$$+ \frac{A(\frac{W}{BW_{TOTAL}})P_{RF}^{pm} + (P_{max}/A.\eta_{PA}) + P_{TRANS_R}}{(1 - \sigma_{DC,R})(1 - \sigma_{MS,R})(1 - \sigma_{optical})} \qquad (21)$$

Then the total power consumed by all active BBUs and RRHs in a C-RAN network can be modelled as

$$P_{supply} = \sum_{m=1}^{M} \left( P_{BBU} + \sum_{n \in Z_m} P_{RRH} \right) \qquad (22)$$

where M represents the number of active BBUs in the network and $Z_m$ represents the list of RRHs handled by $BBU_m$

# 7 CELL DIFFERENTIATION AND INTEGRATION (CDI) ALGORITHM

According to the intuitive analysis above, a CDI algorithm is proposed in this section and Fig. 4. Network information is collected in the first step and analysed for proper cell differentiation and integration. The algorithm seeks to utilise the network resources efficiently by calculating the necessary number of BBUs and RRHs to serve capacity demands at the end of each CDI cycle. Apart from a single BBU required to serve load requirements, proper BBU-RRH configuration is adjusted at the end of optimisation step by comparing the analysed and optimised QoS values. Note that the QoS metrics can be different depending on load intensity and the number of active BBUs and RRHs in the network. For the optimisation part of the algorithm, a Discrete Particle Swarm Optimisation (DPSO) algorithm is developed as an Evolutionary Algorithm (EA) to solve the BBU-RRH configuration problem and is explained in the next section. The optimisation process continues until the CDI cycle is completed. Note that, the CDI algorithm shown in Fig. 4 is triggered at the beginning of each CDI cycle.

The pseudo-codes for semi-static cell differentiation and integration are given in Algorithm 1 and Algorithm 2, respectively. An important consideration is the first association of RRHs to the required number of BBUs during cell differentiation and integration, before identifying a proper BBU-RRH mapping in the optimisation phase. Algorithm 4 and 5 are supporting algorithms for Algorithm 1, and 2 which covers all possible cases of initial BBU-RRH assignment during differentiation or integration of cells along with cases where the number of BBUs are increased, decreased or remain unchanged. The initial BBU-RRH mapping is necessary for utilising the available BBU resources in an efficient manner so as to prevent high blocking rate. The blocking rate of the network at time $t$ can be measured as

$$\text{Blocking rate} = \left[ 1 - \frac{\sum_{m=1}^{M} \sum_{k=1}^{K} I_{m,k}(t)}{K} \right] \times 100 \qquad (23)$$

where $I_{m,k}(t)$ as discussed earlier, is a binary indicator such that $I_{m,k} = 1$, if user $k$ is served by $BBU_m$ at time $t$. Note that, users are served based on the choice of scheduler used
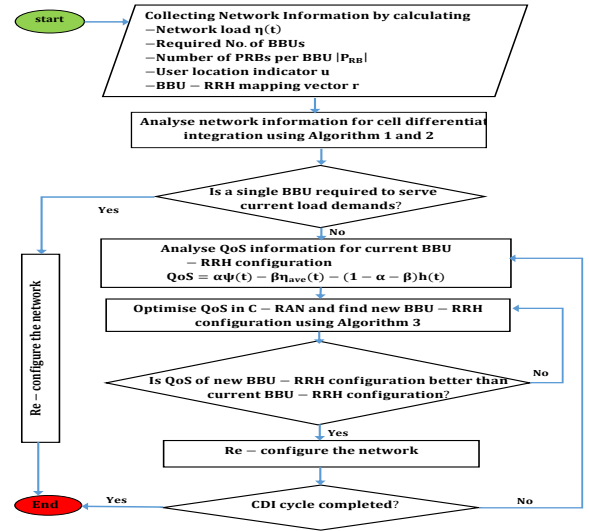


Fig. 4. Block Diagram of CDI Algorithm for one CDI cycle

by a BBU. Moreover, the amount of resource shortage (or PRB shortage) in the network based on users PRB demand can be estimated as follows

$$\text{Resource Shortage} = \sum_{m=1}^{M} \max \left[ (\eta_m(t) - 1), 0 \right] \times 100 \qquad (24)$$

Note that, the CDI algorithm triggers Algorithm 1 and Algorithm 2 sequentially, i.e., Algorithm 2 is triggered immediately after the Algorithm 1 is executed. In the interest of simplicity and understanding, the CDI algorithm is divided into separate pseudo-codes.

## 7.1 Discrete Particle Swarm Optimisation (DPSO)

PSO utilises a population (or swarm) of particles, where each individual particle represents a solution [31], namely BBU-RRH association vector **r** defining the BBU-RRH configuration. As the QoS represented in (14) is considered as the main objective function, PSO seeks to maximise the QoS function by finding the best solution vector $\{r_{11}, r_{12}, ..., r_{in}\}$. PSO utilises a group of particles (or solutions) to probe the solution space in a random way with different velocities. To direct the particles to their best fitness values, the velocity of each particle is changed stochastically at each iteration. The velocity update of each particle $j$ depends on the historical best position experience (pbest) of the particle itself and the best location experience of neighbouring particles i.e., the global best position (gbest) [32] and is given as

$$v_j^I = w v_j^{I-1} + c_1 \varepsilon_1 \left( \text{pbest}_j^I - x_j^I \right) + c_2 \varepsilon_2 (\text{gbest}_j^I - x_j^I)$$
$$1 \le j \le |\Delta| \qquad (25)$$

where $|\Delta|$ represents the population (or swarm) of particles and I represents the Iteration number. $x_j^I$ is the current position of particle $j$ in iteration I and $\varepsilon_1, \varepsilon_2$ are random numbers between 0 and 1. Both $c_1$ and $c_2$ are acceleration

**Algorithm 1:** Pseudo-code for Semi-static Cell Differentiation

   **Input** : Current network load $\eta(t)$ from (7)
            BBU-RRH mapping vector **r**
            Required number of BBUs from (8)

**1**   **if** *No. of active BBUs =1* **then**
**2**    **if** $\eta(t) \geq |P_{\mathrm{RB}}|$ **then**
**3**     -Activate required No. of BBUs
**4**     -Differentiate cell into tier-2 RRH structure by BBU-RRH mapping using Algorithm 4
**5**     -Update BBU-RRH mapping vector **r**
**6**     **for** *i=1 to C* **do**
**7**      -Select set $S_i$
**8**      -Compute $\eta_{\mathrm{RRH}_{i1}}(t)$ from (9)
**9**      **if** $\eta_{\mathrm{RRH}_{i1}}(t) > |P_{\mathrm{RB}}|$ **then**
**10**       - R$\leftarrow S_i$ {Add $S_i$ to R}
**11**       -Diffentiate cell $C_i$ by activating all RRHs in $S_i$ an map them to BBUs according to Algorithm 4.
**12**       -Update BBU-RRH mapping vector **r**.
**13**      **end**
**14**     **end**
**15**    **else**
**16**     -No cell differentiation required.
**17**     -Tier-3 RRH structure remains.
**18**    **end**
**19** **else**
**20**    **if** *No. of active BBUs ≤ No. of required BBUs* **then**
**21**     **if** *All possible RRHs deployed in the network are active* **then**
**22**      -Activate the required No. of BBUs.
**23**      -Cells can not be differentiated further.
**24**      -Update BBU-RRH mapping vector **r**
**25**     **else**
**26**      -Activate required number of BBUs
**27**      **for** *i= 1 to C* **do**
**28**       -Select set $S_i$
**29**       -Compute $\eta_{\mathrm{RRH}_{i1}}(t)$ from (9)
**30**       **if** $\eta_{\mathrm{RRH}_{i1}}(t) > |P_{\mathrm{RB}}|$ **then**
**31**        - R$\leftarrow S_i$ {Add $S_i$ to List R}
**32**        -Differentiate cell $C_i$ further to tier-1 RRH structure by mapping newly activated RRHs to active BBUs using Algorithm 4
**33**        -Update BBU-RRH mapping vector **r**
**34**       **end**
**35**      **end**
**36**     **end**
**37**    **end**
**38** **end**

I + 1 will be:

$$x_j^{\mathrm{I}+1} = x_j^{\mathrm{I}} + \mathrm{v}_j^{\mathrm{I}} \qquad (26)$$

PSO terminates if a stopping criterion is satisfied, e.g. after reaching a predefined number of iterations $I_{max}$. Since the solution vector, **r** (or particle) should be real-valued, the standard PSO algorithm can not be applied to solving this discrete optimisation problem. In this paper, a Discrete Particle Swarm Optimisation (DPSO) is developed to solve the QoS maximisation problem defined in (14). The pseudo code of DPSO is given in Algorithm 3

**Algorithm 2:** Pseudo-code for Semi-static Cell Integration

   **Input** : Current network load $\eta(t)$ from (7)
            BBU-RRH mapping vector **r**
            Required number of BBUs from (8)

**1** **if** *No. of active BBUs =1* **then**
**2**    -No cell integration required.
**3**    -A high-power BS serves the geographical area.
**4** **else**
**5**    **if** *No.of required BBUs=1* **then**
**6**     -Integrate all cells into tier-3 RRH structure, i.e., a high power BS should serve the geographical area.
**7**     -Switch-off remaining BBUs.
**8**     -Update BBU-RRH mapping vector **r**.
**9**    **else**
**10**     **for** *i=1 to C* **do**
**11**      -Select set $S_i$
**12**      **for** *j=1 to end of $S_i$* **do**
**13**       -Compute load $\eta_{\mathrm{RRH}_{ij}}(t)$ from (9)
**14**       -Sum=Sum+$\eta_{\mathrm{RRH}_{ij}}(t)$
**15**      **end**
**16**      **if** *Sum ≤ $P_{\mathrm{RB}}$* **then**
**17**       -Integrate all cells by switching-off all RRHs in set $S_i$ except RRH$_{i1}$.
**18**       -Offload RRHs to required number of BBUs according to Algorithm 5.
**19**       -Update BBU-RRH mapping vector **r**.
**20**      **end**
**21**     **end**
**22**     -Run Algorithm 5 {Case of BBU reduction and no integration}
**23**    **end**
**24** **end**

## 8   COMPUTATIONAL RESULTS AND ANALYSIS

To make the simulation more realistic, the user arrivals in Fig. 6 follows a Poisson process with rate $\lambda$. However, due to the dynamic spatial and temporal nature of user traffic, the user arrival is modelled as a time-inhomogeneous process. This is achieved by multiplying the time-homogeneous Poisson process with traffic intensity parameter $\lambda$ and the rate function $f(t)$ shown in Fig. 5. The rate function is unit-less and reshapes the traffic from constant intensity to an analogous time varying profile that reflects typical traffic patterns in a real cellular network. If users arrive in the system following a Poisson process with intensity $\lambda$

constants that pulls the particle towards best position. Values in the range 0-5 are chosen for $c_1$ and $c_2$. The inertial weight $w$ represents the effect of preceding velocity on the updated velocity. Choosing an optimum value for $w$ can assist a balanced proportion between global and local exploration of the search space. Usually values between 0-1 are selected for $w$ [33]. A value of 0.9 for $w$ is selected in this paper. The new position of particle $j$ for the next iteration

**Algorithm 3:** Discrete Particle Swarm Optimisation (DPSO) Algorithm

---

1  -I=0;
2  -Generate initial Swarm with random position and velocity $(r_1^I, r_2^I, ..., r_{|\Delta|}^I)$.
3  **for** $i = 1$ *to* $|\Delta|$ **do**
4  $\quad$ {Initialise best positions of each particle}
5  $\quad$ pbest$_i$=r$_i^I$
6  **end**
7  -QoS=0;
8  -{Find QoS of each particle using (14) i.e.,}
9  **for** *i=1 to* $|\Delta|$ **do**
10 $\quad$ -Select r$_i^I$ from pbest$_i$
11 $\quad$ **if** $f(r_i^I) > QoS$ **then**
12 $\quad\quad$ QoS=$f(r_i^I)$
13 $\quad$ **end**
14 **end**
15 gbest=QoS;
16 -Update positions and velocities of all particles in the swarm using equation (25) and (26)
17 **while** $I < I_{max}$ **do**
18 $\quad$ **for** *i=1 to* $|\Delta|$ **do**
19 $\quad\quad$ -Select $r_i^I$ from the swarm
20 $\quad\quad$ $F_1=f(r_i^I)$
21 $\quad\quad$ -Select $r_i^I$ from pbest
22 $\quad\quad$ $F_2 = f(r_i^I)$
23 $\quad\quad$ **if** $F_1 \geq F_2$ **then**
24 $\quad\quad\quad$ pbest$_i = r_i^I$
25 $\quad\quad\quad$ QoS=$F_1$
26 $\quad\quad\quad$ **if** $QoS>gbest$ **then**
27 $\quad\quad\quad\quad$ gbest=QoS;
28 $\quad\quad\quad\quad$ $x = i$;
29 $\quad\quad\quad$ **end**
30 $\quad\quad$ **end**
31 $\quad\quad$ -Update positions and velocities of all particles in the swarm using equation (25) and (26)
32 $\quad$ **end**
33 $\quad$ I=I+1;
34 **end**

---

users/min, with a constant service time of $h$ (60 sec), then the number of users at time $t$ is calculated as $K(t) = \chi h f(t)$. Where $\chi \sim Poiss(\lambda)$ is a random variable with mean $\lambda$ (i.e., $\lambda = 200$). Moreover, different data rate requirements are assumed for end users based on 3GPP standard simulation parameters [34] i.e., 4-25 kbps for audio, 32-384 kbps for video, 28.8 kbps for data, and 60 kbps for real-time gaming services. Based on uniform user distribution and network load shown in Fig. 6, an actual number of active BBUs and RRHs with respect to time is shown in Fig. 7.

The BBU-RRH association vector $\mathbf{r} = \{r_{11}, r_{12}, ..., r_{in}\}$ is maintained and updated after each CDI cycle. Newly activated RRHs and BBUs in the network are mapped according to Algorithm 4 and 5. In this paper, a maximum of 49 RRHs and 5 BBUs are deployed in the network to support semi-static cell differentiation and integration. The initial BBU-RRH mapping at the beginning of a CDI cycle might degrade the network QoS. Therefore, dynamic BBU-
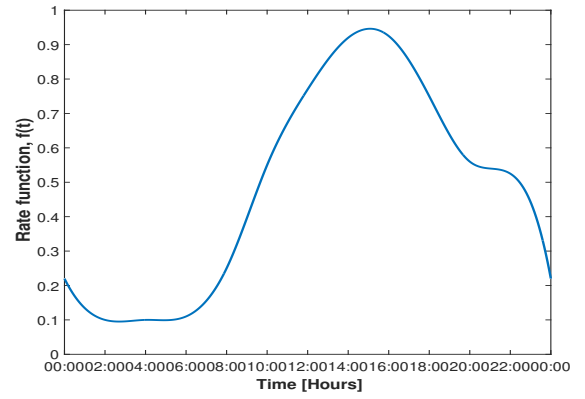


Fig. 5. Rate function for time in-homogeneous user arrivals

RRH mapping is proposed to identify proper BBU-RRH mapping.

Before going to a more thorough analysis of the proposed CDI concept, the efficiency of DPSO over two different problem scenarios, P$_1$, P$_2$, and compared with Exhaustive Search (ES) algorithm . Both scenarios consists of 5 active BBUs with 19 active RRHs including two differentiated cells (Tier 1, level 2, RRH structure) for P$_1$, and 49 active RRHs (Tier 1, level 7, RRH structure) for P$_2$, respectively. The aim is to analyse DPSO performance for small and large networks. User distribution within each cell is uniform where 6 and 25 users are considered for non-dense and high dense cells, respectively.
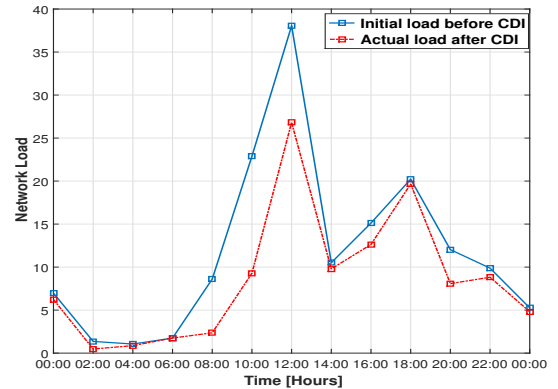


Fig. 6. Actual network load with respect to time

For Monte Carlo analysis, the DPSO and ES algorithms are repeated 50 times with different initial BBU-RRH settings for each problem and results obtained are averaged. The load fairness index, averaged network load, and handover index are represented in Figs 9, 10 and 11, respectively, over 200 iterations for both P$_1$ and P$_2$. The optimum values shown in the figures and Table.2, are achieved by exhaustively searching for all possible solutions N$^M$) using ES algorithm, which helps in demonstrating the improvement in each iteration of the DPSO algorithm. Note that, ES algorithm is independent of iterations.

Fig. 8 shows that the DPSO algorithm converges to the optimum solution in P$_1$ with a Convergence Rate (CR) of
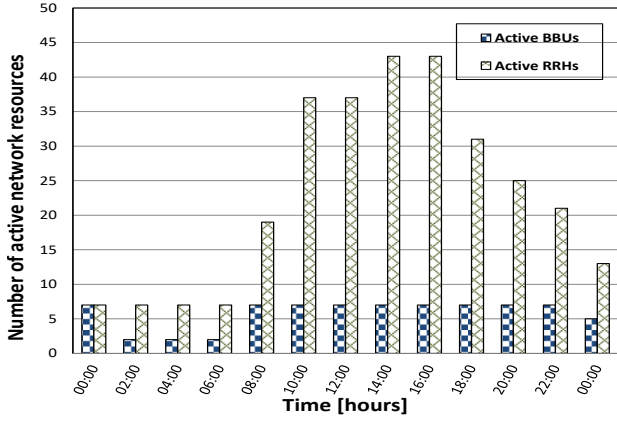
Fig. 7. Number of active BBUs and RRHs with respect to network load/time

TABLE 2
Computational Results for DPSO and ES

|  |  | $P_1$ (19 RRH) | $P_2$ (49 RRH) |
|---|---|---|---|
| Quality of Service | DPSO | 0.599142 | 0.588970793 |
|  | ES | 0.599142 | 0.592940793 |
| Load Fairness Index | DPSO | 0.984797 | 0.97168 |
|  | ES | 0.984797 | 0.97556 |
| Average Network Load | DPSO | 1.506 | 1.4962 |
|  | ES | 1.506 | 1.4663 |
| Handover Index | DPSO | 0.38095 | 0.38748 |
|  | ES | 0.38095 | 0.383659 |

0.825. Where CR is defined as the number of times, the DPSO finds a best or optimum solution during the entire number of iterations. This implies that over 200 iterations, the optimum solution is achieved 165 times for $P_1$. For $P_2$, the CR of DPSO algorithm is 0.12. However, the optimum solution is not reached over 200 generations. DPSO algorithm achieves the best value 24 times i.e., after 176 iterations and $176 \times |\Delta|$ fitness evaluations, which is still 99.53% of the optimum value achieved by ES algorithm after an enormous $5^{49}$ ($M^N$) fitness evaluations.
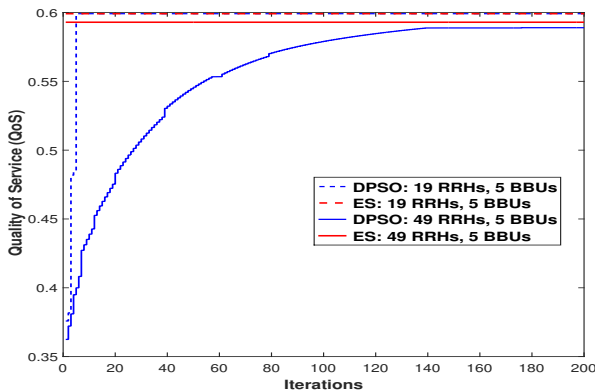


Fig. 8. QoS values for DPSO and ES

Fig. 9 shows that the DPSO algorithm converges to the optimum load fairness index value after $13^{th}$ iteration in $P_1$. However, in $P_2$, the optimum value can not be found over 200 iterations, and the best load fairness index value

is achieved after only 176 iterations and $176 \times |\Delta|$ fitness evaluations, which is 99.57% of the optimum value found by ES algorithm. ES algorithm performs $5^{49}$ fitness evaluations to find the optimum value which is a considerable amount of fitness evaluations.
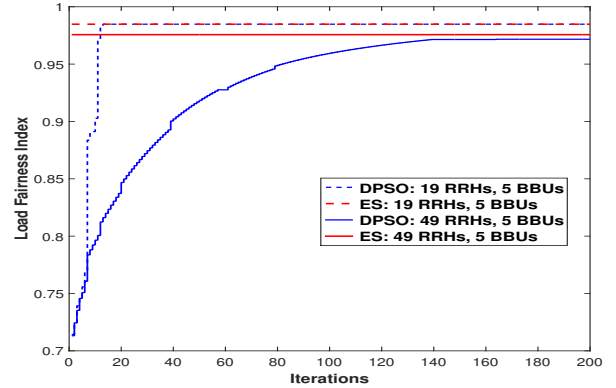


Fig. 9. Load fairness index values for DPSO and ES.

Figs 10 and 11 displays the convergence of DPSO algorithm to the optimum value for average load value and handover index in both $P_1$ and $P_2$. In $P_1$, optimum are achieved after 12 and 38 iterations for average network load and handovers, respectively. For $P_2$, the DPSO algorithm could not find the optimum value over 200 iterations. However, the best possible value achieved for average network load and handover index are 98% and 99.01% of the optimum value found by ES algorithm, respectively. ES algorithm determines the optimum value after performing $5^{49}$ enormous fitness evaluations whereas the DPSO algorithm performs $67 \times |\Delta|$ and $145 \times |\Delta|$ to find the best value for average network load and handover index, respectively. Note that, the $\alpha$ and $\beta$ control parameters in (14) are selected by performing an exhaustive search (ES) algorithm to identify the optimal BBU-RRH setting for $P_1$. Both $\alpha$ and $\beta$ values are orderly set to 0, 0.1, ..., 1 with a constraint $\alpha + \beta \leq 1$ as shown in Fig. 12. An optimal BBU-RRH setting is found using ES algorithm for each pair of $\alpha$ and $\beta$. It is observed that setting a higher value for load fairness index (until $\alpha = 0.8$) not only reduces the resource shortage but also improves network balance. Setting values for $\alpha > 0.8$ results into improper BBU-RRH mapping which implies that maximising network load balance is overly considered compared to minimising average network load and handovers, resulting into an increased resource shortage. This paper considers $\alpha = 0.8$ and $\beta = 0.1$ which means assigning a 10% weight to handover minimisation.

For a more thorough analysis, the proposed CDI concept is compared to a fixed C-RAN scenario (F-CRAN). The BBU cloud holds five BBUs in both cases. However, the fixed C-RAN scenario does not support cell differentiation or integration, and only 7 RRHs serves the entire macrocell coverage area. The dynamic BBU-RRH mapping is enabled in the fixed C-RAN scenario which shows $5^7$ possible BBU-RRH mapping solutions to choose from at the beginning of each CDI cycle. The number of possible BBU-RRH mapping solutions for CDI scenario at the start of each CDI cycle
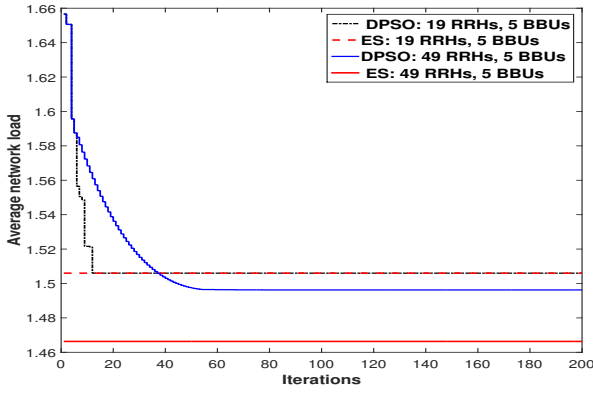
Fig. 10. Average network load for DPSO and ES.

is $M^N$, where M and N represents the number of active BBUs and RRHs, respectively. Moreover, an increasing user arrival is considered in the network with random data rates requirement as explained earlier. However, a Monte-Carlo analysis is performed, where 100 uniformly distributed users are envisaged for each instance, and the average of all distributions are taken into account regarding network load, throughput, blocked users, and resource shortage analysis. Figs 13 and 14 shows the relative performances regarding average blocked users and average network throughput with Proportional Fair (PF) and Round Robin (RR) scheduling techniques. Since the CDI algorithm includes 2 phases of BBU-RRH mapping, i.e., the initial BBU-RRH assignment during cell integration/differentiation and the optimum BBU-RRH setting achieved by DPSO in the second step, the results of both phases are analysed.
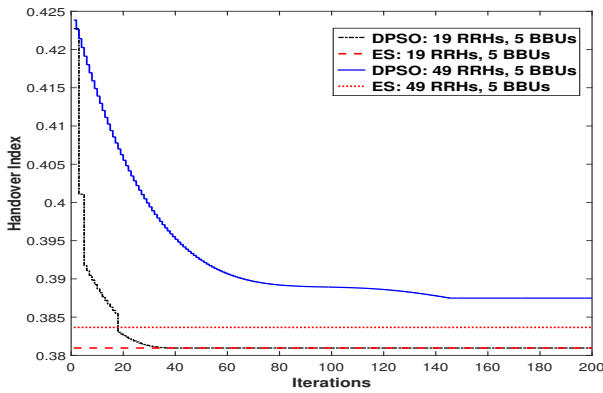


Fig. 11. Average handovers for DPSO and ES.

The simulation results demonstrate the advantage of using CDI-enabled C-RAN (CDI-CRAN) instead of a F-CRAN setting. When a fixed C-RAN is considered, the average blocked users in the network are much higher with significantly lower average throughput, using any scheduling technique, as shown in Figs 13 and 14, provided that the dynamic BBU-RRH mapping is also enabled. However, an interesting observation is the significant drop in the averaged blocked users and the necessary increase in average network throughput in CDI-CRAN compared

**Algorithm 4:** Initial RRH association to active BBUs during cell differentiation.

---

**Input** : List A of newly activated BBUs
List R containing sets of RRHs supporting cell differentiation

1 **if** *A is not empty* **then**
2   **for** *m=1 to No. of active BBUs* **do**
3    -Compute $\eta_m(t)$ from (6)
4    **if** $\eta_m(t) \leq$ *lower limit* **then**
5     A← BBU$_m$\{Add BBU$_m$ to List A\}
6    **end**
7   **end**
8   I=1;
9   **while** *not the end of List R* **do**
10    -Select I$^{th}$ set from list R
11    $m = 1$;
12    **for** *j=1 to end of set $S_i$* **do**
13     **if** $m> |A|$ **then**
14      $m = 1$
15     **end**
16     $BBU_m \leftarrow RRH_{ij}$\{Map $RRH_{ij}$ to $BBU_m$ except $R_{1j}$\}
17     $m = m + 1$;
18    **end**
19    I=I+1;
20   **end**
21 **else**
22   **for** *m=1 to No. of active BBUs* **do**
23    -Compute $\eta_m(t)$ from (6)
24    **if** *lower limit* $\leq \eta_m(t) \leq$ *Upper limit* **then**
25     A← BBU$_m$\{Add BBU$_m$ to A\}
26    **end**
27   **end**
28   **if** *A is still empty* **then**
29    A ← All active BBUs
30   **end**
31   -Sort A in increasing order of BBU loads
32   I=1;
33   **while** *not the end of List R* **do**
34    -Select I$^{th}$ set from List R
35    $m = 1$;
36    **for** *j=1 to end of set $S_i$* **do**
37     **if** $m> |A|$ **then**
38      m=1;
39     **end**
40     BBU$_m$ ← RRH$_{ij}$\{Map RRH$_{ij}$ to BBU$_m$ except RRH$_{1j}$\}
41    **end**
42    I=I+1;
43   **end**
44 **end**

---

to F-CRAN. This indicates that during cell differentiation, an overloaded cell divides into multiple smalls cells, and not only reduces the user to RRH distances but also the PRB demands resulting from high SINR and low path loss values. A further decrease in average network load is observed after proper BBU-RRH mapping, providing a balanced network load across the active BBUs. Note that,

**Algorithm 5:** Initial RRH association to active BBUs during cell integration.

> **Input** : List A of No. of active BBUs
> No. of required BBUs
> BBU-RRH mapping vector r

**1** **if** *No. of required BBUs* $< |A|$ **then**
**2**    **for** *m=1 to* $|A|$ **do**
**3**      **for** *i=1 to C* **do**
**4**        **for** *j=1 to c* **do**
**5**          -Select $\text{RRH}_{ij}$ from BBU-RRH vector **r**
**6**          **if** $RRH_{ij} = m$ **then**
**7**            $Z_m \leftarrow \text{RRH}_{ij}$
**8**            {$Z_m$ is a List of RRHs handled by $\text{BBU}_m$}
**9**          **end**
**10**        **end**
**11**      **end**
**12**    **end**
**13**    -Sort List A in decreasing order of BBU loads
**14**    **for** *m=1 to end of List A* **do**
**15**      **if** *m* $\neq$ *|No. of required BBUs|* **then**
**16**        $\overline{A} \leftarrow \text{BBU}_m$ {$\overline{A}$ is a List of required BBUs}
**17**      **else**
**18**        $\overline{B} \leftarrow \text{BBU}_m$
**19**        {$\overline{B}$ is a List of BBUs to be switched off}
**20**      **end**
**21**    **end**
**22**    -Sort List $\overline{A}$ in increasing order of BBU loads
**23**    **for** *i=1 to end of List* $\overline{B}$ **do**
**24**      -Select $i^{th}$ BBU from List $\overline{B}$
**25**      -Select List $Z_m$ of the $i^{th}$ BBU
**26**      m=1;
**27**      **for** *j=1 to end of* $Z_m$ **do**
**28**        **if** *m*$> |\overline{A}|$ **then**
**29**          m=1;
**30**        **end**
**31**        -Select RRH at j$^{th}$ index in List $Z_m$
**32**        -Select BBU at m$^{th}$ index of List $\overline{A}$
**33**        -$\text{BBU}_m \leftarrow \text{RRH}^j$ {Assign RRH j to BBU m}
**34**        m++
**35**      **end**
**36**    **end**
**37**    -Switch off all BBUs in List $\overline{B}$
**38** **end**



Fig. 12. Resource shortage for different $\alpha$ and $\beta$.

TABLE 3
Comparison results for fixed and CDI-enabled C-RAN

|  | Blocking Rate[%] | | | | Resource Shortage | |
|---|---|---|---|---|---|---|
|  | Initial | | Proper | | Initial | Proper |
|  | PF | RR | PF | RR | | |
| F-CRAN | 35.99 | 81.66 | 35.34 | 81.10 | $16.44 \times 10^3$ | $16.42 \times 10^3$ |
| CDI-CRAN | 26.87 | 67.33 | 25.809 | 62.13 | $38.79 \times 10^2$ | $38.47 \times 10^2$ |

tion, ensuring minimum blocked users until a proper BBU-RRH setting is identified. Note that, the initial BBU-RRH mapping supported by Algorithm 4 and 5, is an important consideration in the overall CDI concept (as explained earlier). About 23.149% reduction in the average number of blocked users with PF scheduler and 20.903% with RR is observed in Fig. 13. Moreover, the average resource shortage drastically decreases in the CDI-CRAN, compared to fixed C-RAN as shown in Table.3 provided that both scenarios have an equal amount of resources available (i.e., 5 BBUs, 5×100 PRBs). A 76.57% decrease in average PRB shortage is estimated with CDI-CRAN compared to F-CRAN.



Fig. 13. Average blocked users for fixed and CDI-enabled C-RAN.

Fig. 15 shows the average power consumed by the C-RAN network for both CDI and fixed setting for different schedulers. Despite the fact that the geographical area is served with more RRHs in CDI-CRAN, the total power consumed by the network is still lower. An average de-

cell differentiation increases the number of RRH interferers in the network. However, RRHs served by the same BBU does not contribute to the overall interference experienced by users served by the same BBU.

From the results shown in Fig. 14, it is observed that the average network throughput increases by 45.53% in the CDI-CRAN compared to F-CRAN, both enabled with PF schedulers. Whereas with RR schedulers, an increase of 42.102% is observed. Moreover, the average throughput difference between initial and optimum BBU-RRH mapping in a CDI-enabled C-RAN, with PF and RR scheduling is 4.0219% and 4.126%, respectively. This indicates efficient resource utilisation during cell differentiation and integra-
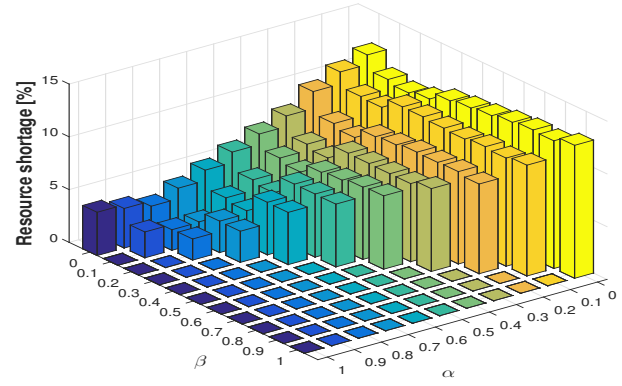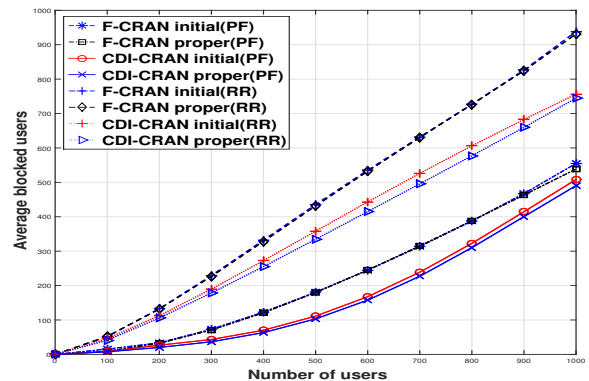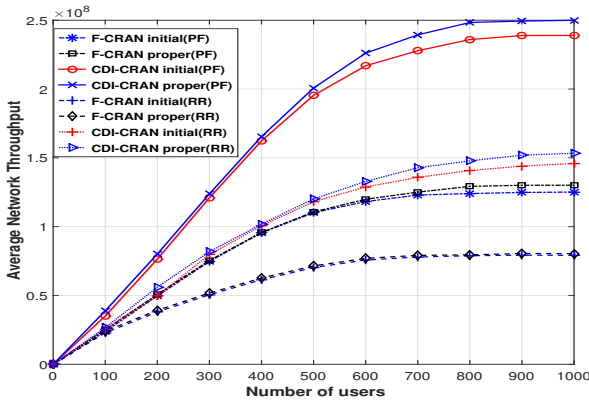
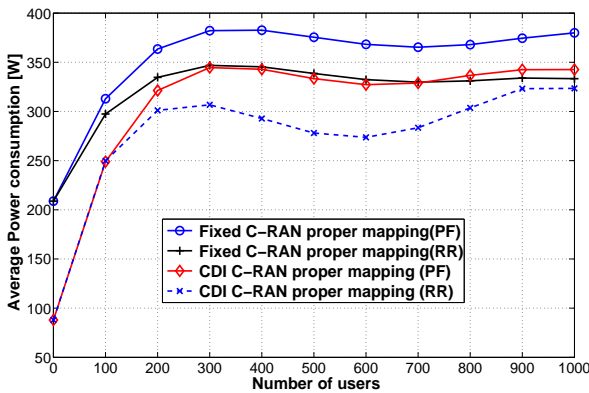Fig. 14. Average network throughput for fixed and CDI-enabled C-RAN.



Fig. 15. Average power consumed by fixed and CDI-enabled C-RAN.

crease of $\approx 15.28\%$ and $\approx 16.02\%$ in the average power consumption is estimated in the CDI-CRAN with PF and RR schedulers, respectively, compared to a fixed C-RAN setting. Fig. 16 shows the SINR thresholds versus the probability of coverage results. The CDI activated C-RAN performs well compared to fixed C-RAN regarding coverage performances for 1000 users, provided that no interference mitigation techniques are applied in this work. Note that, the path-loss models for different tiers of cell differentiation are
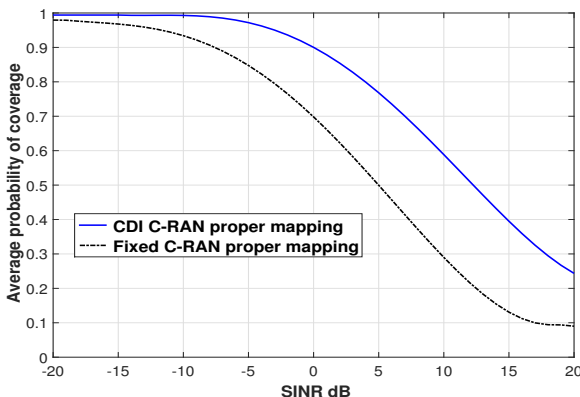
not identical, the probability of coverage still has a linear behaviour for SINR thresholds within the range of 0dB to 5dB for both cases.

## 9 CONCLUSION

The concept of cell differentiation and integration in C-RAN is examined with an objective to utilise network resources efficiently without degrading the overall network QoS. An energy efficient C-RAN network is considered to accommodate traffic by scaling the BBUs and RRHs as well as maintaining a balanced network via proper BBU-RRH mapping, formulated as a constrained integer programming problem. A CDI algorithm is developed for C-RAN and tested for comparison with a fixed C-RAN setting. Computational results based on Monte Carlo analysis shows an average throughput increase of 45.53% with 23.149% decrease in average blocked users and 76.57% reduction in average resource (PRBs) shortage. The CDI algorithm hosts a DPSO algorithm which is developed to find optimum BBU-RRH configuration dynamically. The performance of DPSO is tested and compared to ES. Using two benchmark problems, the DPSO delivered noticeably faster convergence compared to ES, which makes the CDI algorithm more reliable for a self-organised C-RAN. Moreover, the power model for C-RAN is proposed to estimate the overall network power consumption. It is noticed that despite deploying a higher number of RRHs (49) in a given geographical area for CDI enabled C-RAN, the power consumption of a fixed C-RAN for the same geographic area is still higher by $\approx 15.28\%$ and $16.02\%$ for PF and RR schedulers, respectively.

## REFERENCES

[1] T. Q. Quek, M. Peng, O. Simeone, and W. Yu, *Cloud radio access networks: Principles, technologies, and applications*. Cambridge University Press, 2017.

[2] M. Peng, Y. Sun, X. Li, Z. Mao, and C. Wang, "Recent Advances in Cloud Radio Access Networks: System Architectures, Key Techniques, and Open Issues," *IEEE Communications Surveys Tutorials*, vol. 18, no. 3, pp. 2282–2308, thirdquarter 2016.

[3] A. Checko, H. L. Christiansen, Y. Yan, L. Scolari, G. Kardaras, M. S. Berger, and L. Dittmann, "Cloud RAN for Mobile Networks;A Technology Overview," *IEEE Communications Surveys Tutorials*, vol. 17, no. 1, pp. 405–426, Firstquarter 2015.

[4] M. Khan, R. Alhumaima, and H. Al-Raweshidy, "Reducing energy consumption by dynamic resource allocation in C-RAN," in *Networks and Communications (EuCNC), 2015 European Conference on*. IEEE, 2015, pp. 169–174.

[5] Y. Cai, F. R. Yu, and S. Bu, "A decision theoretic approach for clustering and rate allocation in coordinated multi-point (CoMP) networks with delayed channel state information," *Transactions on Emerging Telecommunications Technologies*, vol. 28, no. 1, 2017.

[6] C. Jiang, H. Zhang, Y. Ren, Z. Han, K. C. Chen, and L. Hanzo, "Machine Learning Paradigms for Next-Generation Wireless Networks," *IEEE Wireless Communications*, vol. 24, no. 2, pp. 98–105, April 2017.

[7] X. Huang, G. Xue, R. Yu, and S. Leng, "Joint Scheduling and Beamforming Coordination in Cloud Radio Access Networks With QoS Guarantees," *IEEE Transactions on Vehicular Technology*, vol. 65, no. 7, pp. 5449–5460, July 2016.

[8] K. Wang, W. Zhou, and S. Mao, "On Joint BBU/RRH Resource Allocation in Heterogeneous Cloud-RANs," *IEEE Internet of Things Journal*, vol. PP, no. 99, pp. 1–1, 2017.

[9] Y. Shi, J. Zhang, and K. B. Letaief, "Group Sparse Beamforming for Green Cloud-RAN," *IEEE Transactions on Wireless Communications*, vol. 13, no. 5, pp. 2809–2823, May 2014.

Fig. 16. Probability of coverage versus SINR threshold

[10] S. Namba, T. Warabino, and S. Kaneko, "BBU-RRH switching schemes for centralized RAN," in *Communications and Networking in China (CHINACOM), 2012 7th International ICST Conference on*. IEEE, 2012, pp. 762–766.

[11] K. Sundaresan, M. Y. Arslan, S. Singh, S. Rangarajan, and S. V. Krishnamurthy, "FluidNet: a flexible cloud-based radio access network for small cells," *IEEE/ACM Transactions on Networking*, vol. 24, no. 2, pp. 915–928, 2016.

[12] Y. S. Chen, W. L. Chiang, and M. C. Shih, "A Dynamic BBU-RRH Mapping Scheme Using Borrow-and-Lend Approach in Cloud Radio Access Networks," *IEEE Systems Journal*, vol. PP, no. 99, pp. 1–12, 2017.

[13] C. Ran, S. Wang, and C. Wang, "Optimal load balancing in cloud radio access networks," in *2015 IEEE Wireless Communications and Networking Conference (WCNC)*, March 2015, pp. 1006–1011.

[14] M. Awais, A. Ahmed, M. Naeem, M. Iqbal, W. Ejaz, A. Anpalagan, and H. S. Kim, "Efficient Joint User Association and Resource Allocation for Cloud Radio Access Networks," *IEEE Access*, vol. 5, pp. 1439–1448, 2017.

[15] M. Khan, R. S. Alhumaima, and H. S. Al-Raweshidy, "QoS-Aware Dynamic RRH Allocation in a Self-Optimized Cloud Radio Access Network With RRH Proximity Constraint," *IEEE Transactions on Network and Service Management*, vol. 14, no. 3, pp. 730–744, Sept 2017.

[16] W. He, J. Gong, X. Su, J. Zeng, X. Xu, and L. Xiao, "SDN-Enabled C-RAN? An Intelligent Radio Access Network Architecture," in *New Advances in Information Systems and Technologies*. Springer, 2016, pp. 311–316.

[17] M. Condoluci, T. Mahmoodi, and G. Araniti, "Software-Defined networking and network Function Virtualization for C-RAN Systems," *5G Radio Access Networks: Centralized RAN, Cloud-RAN and Virtualization of Small Cells*, p. 117, 2017.

[18] S. Gu, Z. Li, C. Wu, and H. Zhang, "Virtualized Resource Sharing in Cloud Radio Access Networks Through Truthful Mechanisms," *IEEE Transactions on Communications*, vol. 65, no. 3, pp. 1105–1118, March 2017.

[19] H. Dahrouj, A. Douik, O. Dhifallah, T. Y. Al-Naffouri, and M. S. Alouini, "Resource allocation in heterogeneous cloud radio access networks: advances and challenges," *IEEE Wireless Communications*, vol. 22, no. 3, pp. 66–73, June 2015.

[20] J. Zhang, R. Zhang, G. Li, and L. Hanzo, "Distributed Antenna Systems in Fractional-Frequency-Reuse-Aided Cellular Networks," *IEEE Transactions on Vehicular Technology*, vol. 62, no. 3, pp. 1340–1349, March 2013.

[21] M. K. Simon and M.-S. Alouini, *Digital communication over fading channels*. John Wiley & Sons, 2005, vol. 95.

[22] C. Bouras, G. Diles, V. Kokkinos, K. Kontodimas, and A. Papazois, "A simulation framework for evaluating interference mitigation techniques in heterogeneous cellular environments," *Wireless personal communications*, vol. 77, no. 2, pp. 1213–1237, 2014.

[23] H. Zhang, C. Jiang, J. Cheng, and V. C. M. Leung, "Cooperative interference mitigation and handover management for heterogeneous cloud small cell networks," *IEEE Wireless Communications*, vol. 22, no. 3, pp. 92–99, June 2015.

[24] R. S. Alhumaima, M. Khan, and H. S. Al-Raweshidy, "Component and parameterised power model for cloud radio access network," *IET Communications*, vol. 10, no. 7, pp. 745–752, 2016.

[25] C. Desset, B. Debaillie, V. Giannini, A. Fehske, G. Auer, H. Holtkamp, W. Wajda, D. Sabella, F. Richter, M. J. Gonzalez *et al.*, "Flexible power modeling of lte base stations," in *Wireless Communications and Networking Conference (WCNC), 2012 IEEE*. IEEE, 2012, pp. 2858–2862.

[26] H. A. Holtkamp, "Enhancing the energy efficiency of radio base stations," Ph.D. dissertation, University of Edinburgh, 2014.

[27] R. S. Tucker and K. Hinton, "Energy consumption and energy density in optical and electronic signal processing," *IEEE Photonics Journal*, vol. 3, no. 5, pp. 821–833, 2011.

[28] K.-L. Lee, B. Sedighi, R. S. Tucker, H. K. Chow, and P. Vetter, "Energy efficiency of optical transceivers in fiber access networks [invited]," *Journal of Optical Communications and Networking*, vol. 4, no. 9, pp. A59–A68, 2012.

[29] A. Chatzipapas, S. Alouf, and V. Mancuso, "On the minimization of power consumption in base stations using on/off power amplifiers," in *Online conference on green communications (GreenCom), 2011 IEEE*. IEEE, 2011, pp. 18–23.

[30] G. Auer, V. Giannini, C. Desset, I. Godor, P. Skillermark, M. Olsson, M. A. Imran, D. Sabella, M. J. Gonzalez, O. Blume *et al.*, "How much energy is needed to run a wireless network?" *IEEE Wireless Communications*, vol. 18, no. 5, 2011.

[31] A. Kaveh, "Particle swarm optimization," in *Advances in Metaheuristic Algorithms for Optimal Design of Structures*. Springer, 2017, pp. 11–43.

[32] A. Passaro and A. Starita, "Particle swarm optimization for multimodal functions: a clustering approach," *Journal of Artificial Evolution and Applications*, vol. 2008, 2008.

[33] J. Vesterstrom and R. Thomsen, "A comparative study of differential evolution, particle swarm optimization, and evolutionary algorithms on numerical benchmark problems," in *Evolutionary Computation, 2004. CEC2004. Congress on*, vol. 2. IEEE, 2004, pp. 1980–1987.

[34] 3GPP, "Technical Specification Group Services and System Aspects;Services and service capabilities (Release 13) ," 3rd Generation Partnership Project (3GPP), TS V13.0.0, Dec. 2015.

**Zainab Fakhri** received her BSc degree in electrical engineering from Al-Mustansiriya University Baghdad (2004) and her MSc from University of Technology Baghdad (2006). She is currently working on her PhD at Brunel University London. Her research interests include cloud radio access network, self-organized networks and millimeter wave communications.

**Muhammad Khan** received the B.Eng. degree in Electronics Engineering from COMSATS Institute of Information Technology (CIIT), Abbottabad, Pakistan, in 2008. He is currently pursuing the Ph.D. degree in wireless communications with Brunel University London, UK, under the supervision of Prof. Hamed Al-Raweshidy. He joined the Department of Computer Science, Abdul Wali Khan University Mardan, Pakistan, as a Lecturer in 2009. His main research interest is next generation wireless communications and Cloud Radio Access Networks, particularly in Self-Optimisation and Load Balancing.

**Firas Sabir** is an Associate Professor in computer engineering department university of Baghdad. He received his Ph.D. Degree Electrical and Electronic Engineering from the University of Technology, Baghdad (2008). He is currently a visitor researcher at the Wireless Networks and Communications Centre (WNCC) at Brunel University London,UK. His areas of specialty and interest are next Generation of mobile communication, cloud radio access networks and self-organised networks
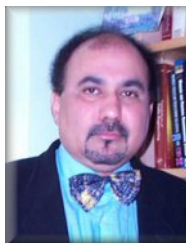
**Hamed Al-Raweshidy** is professor of Communications Engineering and has been awarded his PhD in 1991 from Strathclyde University in Glasgow/UK. He was with Space and Astronomy Research Centre/Iraq, PerkinElmer/USA, Carl Zeiss/Germany, British Telecom/UK, Oxford University, Manchester Met.University and Kent University. Professor Al-Raweshidy is currently the Director of the Wireless Networks and Communications Centre (WNCC) and Director of PG studies (ECE) at Brunel University, London, UK. His current research area is 5G and beyond such as C-RAN, SDN, IoT, M2M and Radio over Fibre.